Effects of micro-knurling and femtosecond laser micro texturing on aluminum long-term surface wettability

Synthia Divin-Mariotti, Pierrick Amieux, Alina Pascale-Hamri, Virginie Auger, Guillaume Kermouche, Frederic Valiorgue, Stéphane Valette

"Effects of micro-knurling and femtosecond laser micro texturing on aluminum long-term surface wettability"

Synthia Divin-Mariotti[a,*], Pierrick Amieux[b], Alina Hamri[b], Virginie Auger[c], Guillaume Kermouche[d], Frédéric Valiorgue[e], Stéphane Valette[a,*]

[a] Univ Lyon, Ecole Centrale de Lyon, Laboratoire de Tribologie et Dynamique des Systèmes, UMR 5513, 36 avenue Guy de Collongue, 69134 Ecully Cedex, France

[b] MANUTECH-USD, 20 rue du Professeur Benoît Lauras, 42000 Saint-Etienne, France

[c] CETIM, 7 Rue de la Presse, 42000 Saint-Étienne, France

[d] Laboratoire LGF, Ecole des Mines de Saint Etienne, Centre SMS, UMR 5307, 158 Cours Fauriel, 42023 Saint-Étienne, France

[e] Laboratoire de Tribologie et Dynamique des Systèmes, Ecole Nationale d'Ingénieurs de Saint-Etienne, UMR CNRS 5513, 58 Rue Jean Parot, 42100 Saint-Étienne, France

*Corresponding author. E-mail address: synthia.divin@ec-lyon.fr (Synthia DIVIN-MARIOTTI), stephane.valette@ec-lyon.fr (Stéphane VALETTE)

Abstract

A comparison of the long-term evolution of a femtosecond laser and the mechanical knurling texturing of aluminum surfaces is performed. Both the femtosecond laser and knurling textured surfaces present similar topographical parameters in the micrometer range. To compare both texturing approaches, long-term physico-chemical characterizations are performed. These characterizations consist of wettability measurements and XPS analyses as a function of time following the texturing operations. The evolution of the wetting properties over time for the femtosecond laser textured surface is explained through chemical modifications of the extreme surface. High-resolution XPS spectra highlight a C-C/C-O bond ratio evolution over time. This time evolution of the chemical bonds of the extreme surface is corroborated with the static contact angle evolution. On the contrary, the mechanically knurled surfaces present a steady state after texturing: neither the evolution of the wetting properties nor the chemical composition of the extreme surface is measured.

Keywords

Femtosecond laser, Knurling, Aluminum, Micrometric texturing, Long-term wettability, Chemical evolution

1. Introduction

Surface texturing has been widely developed in the past few decades to tailor surface wettability and/or tribological properties [1-6]. Micrometric texturing can be obtained by means of several methods; lithography, ion etching, micro-casting or material ablation using a femtosecond laser are the most emblematic ones [7]. The latter is promising regarding industrial applications as it is able to produce a broad range of patterns at different scales, without a heat affected zone and mainly in a one-single step process [8-13]. However, it can lead to changes in surface chemistry and thus affect surface wettability [14-18]. For instance, Bizi-Bandoki *et al.* have shown that a hydrophilic behavior is observed on steels and Al alloys immediately after laser processing. A transition from hydrophilicity to hydrophobicity is then observed in the few days following laser texturing [16-18]. Sciancalepore *et al.* relate this time-dependent behavior to the increase of carbon content [19]. Consequently, this kind of process requires further investigation to quantify the respective roles of surface reactivity and surface texturing on wettability.

To overcome this issue, it would be necessary to develop other flexible technologies that would not affect surface reactivity. Knurling appeared as a good option. It is a mechanical process that has been used successfully for years to produce millimetric textured surfaces that are known to increase adherence strength [20-22]. It is based on the negative replication of the surface texture of a knurl on the surface to be textured, using rolling with no sliding kinematics. This kind of process should not affect the surface reactivity as it does not induce material ablation or temperature rises. However, surface micro texturing based on a knurling operation has never been investigated to create patterns at a micrometric scale. Micro-knurling texturing might also offer a fast and cheap alternative to femtosecond laser processing.

The aim of this paper is to prove the efficiency of the micro-knurling process to produce micro patterns and to compare the resulting surface topography, wettability and reactivity to those obtained after using a femtosecond laser process on aluminum [23-26]. For that

purpose, long-term physico-chemical characterizations are performed. These characterizations consist in wettability measurements and XPS analyses as a function of time, subsequent to the texturing operations.

2. Materials and methods

2.1 Materials

Surface texturing was performed on Al1050 (Table 1) with a hardness of 34 HV. The raw material was a laminated plate of 1.5 mm thickness.

Al	Cu	Mg	Mn	Fe	Si	Zn	Ti
99.5	0.05	0.05	0.05	0.4	0.25	0.07	0.05

Table 1: Composition of 1050 aluminum in %

Six 14x14mm samples were cut out (Figure 1: Sketch of Al samples.). The samples were manually polished with 1µm silica suspension resulting in a mirror-like surface finish with an average roughness R_a of about 50nm. Three samples were dedicated to XPS tests and were stored in ambient air without being submitted to any cleaning process between each measurement. Three samples were dedicated to wetting tests and were cleaned with acetone immersion during ten minutes, rinsed with distilled water and dried with hot air before each measurement [27-28]. The wetting and XPS samples were stored in ambient air with controllable hygrometry between each measurement (Figure 2: Samples studied matrix.).

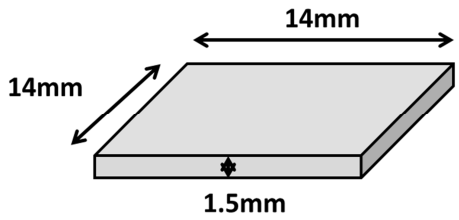

Figure 1: Sketch of Al samples.

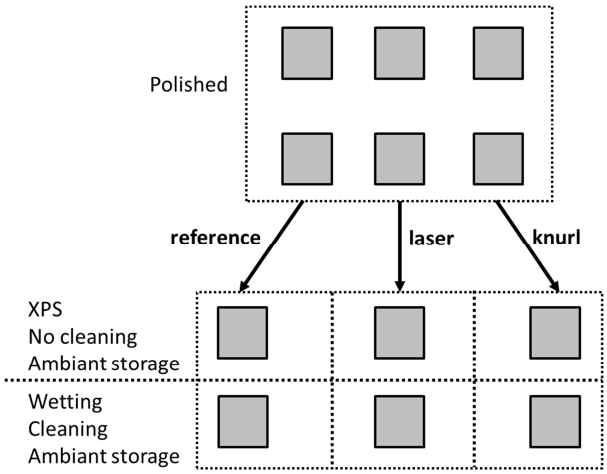

Figure 2: Samples studied matrix.

2.2 Surface texturing

2.2.1 Micro-knurling process

Micro-knurling is based on two steps. First the knurl must be textured with the chosen morphology. Then the surface is textured using a rolling without sliding motion of the knurl. Contrary to the femtosecond laser process based on ablation, knurling micro-patterns result from local plastic deformations.

The knurl was machined from 42CD4 steel alloy. It was belt finished and then nitrided to reach a hardness close to 800HV. The knurl surface texture was obtained using a femtosecond laser. The micro-patterns consist of grooves with a wavelength period of λ=27µm, a mean depth of z=7µm and a top-flat width of the grooves W=14µm (Figure 3 : Micro-knurling surface process principle: a) experimental setup installed on a 5-axis machining center b) surface confocal topography top view and c) cross section profilec), which are convenient for replication by micro-knurling. These micro-patterns have been chosen to promote a hydrophilic behavior as shown in the literature [29-31].The knurl was installed on a 5-axis machining center, through a specific set-up. The latter involves a spring that transforms the spindle vertical displacement into an applied load. This spring function was created by means of spring blades and the resulting load was measured with a kistler dynamometer (Figure 3a).

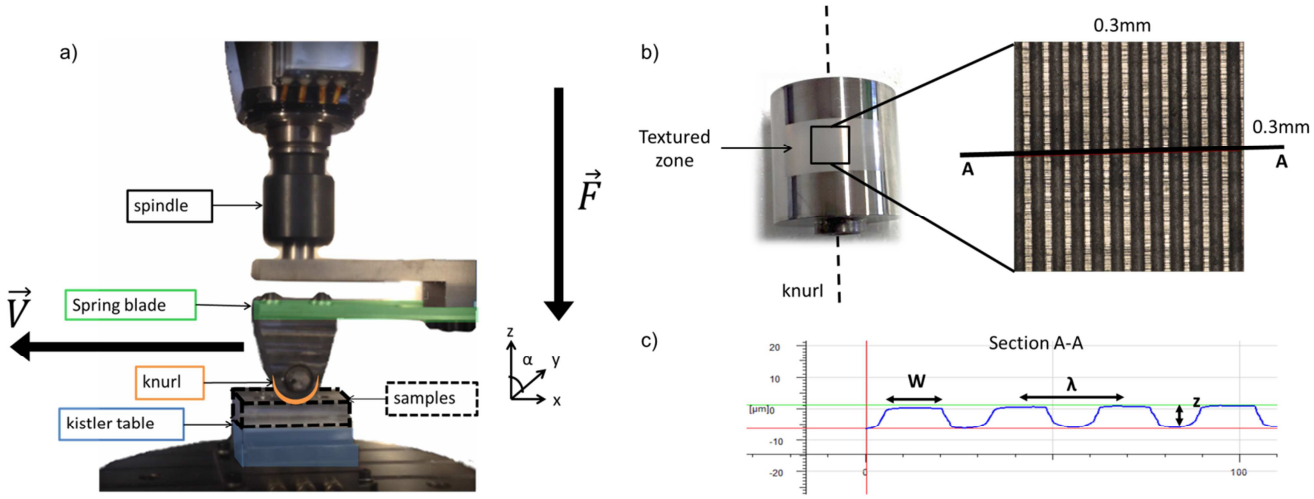

Figure 3 : Micro-knurling surface process principle: a) experimental setup installed on a 5-axis machining center b) surface confocal topography top view and c) cross section profile.

2.2.2 Laser processing

Laser surface texturing was performed with an ultrashort-pulse laser process (Ultrafast Surface Design Platform, MANUTECH-USD). The laser was a high power fiber laser system (Tangor HP, Amplitude system) delivering ultrashort pulses around 400fs long and 1030 nm wavelength pulses at a repetition rate of 100kHz. Assuming a laser power of 680mW, a laser repetition rate of 100 kHz and a Gaussian beam profile, the fluence was about 1.6 $J.cm^{-2}$. The surface texturing was ensured by the displacement of the sample fixed on a motorized three-axis system. To obtain parallel microscale grooves, a spot of Φ=33µm diameter and a longitudinal spot overlap of δ=5µm at a 0.5 $m.s^{-1}$ scanning speed in the direction of the grooves was made. A lateral spot overlap of Δ=27 µm was imposed (Figure 4). This process allowed minimizing roughness irregularities at the bottom of the grooves.

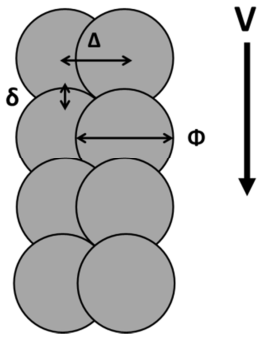

Figure 4: Scheme of the laser scanning process using the overlap distance Δ, the interval δ and the spot size Φ.

2.3 Surface characterizations

The effects of laser and micro-knurling texturing on the surface morphology were investigated by means of confocal microscopy (model Alicona InfiniteFocusG5) and surface physico-chemistry by X-ray Photoelectron Spectrometry (XPS) and wetting. Measurements were made in the first 4 days, and then on the 9^{th}, 11^{th}, 15^{th}, 21^{st} and the 53^{rd} days after texturing.

X-ray photoelectron spectroscopy (XPS) measurements (model Ulvac-Phi Versaprobe II) were performed to quantify the elementary composition of the surfaces with a monochromatic Al Kα source. The survey spectra were made from 0 to 1100eV with an incrementing of 0.8eV during 0.2s and with a pass energy of 187.85eV. In order to rid the peak shifts from the remaining charge effect, the binding energy of all spectra was scaled using the main peak of carbon C1s at 284.8 eV as reference. High resolution XPS analysis allows a peak de-convolution and thus the calculation of relative chemical bonds involved with each element. The high resolution spectra were made from 65 to 80eV for Al2p, from 525 to 540eV for O1s and from 278 to 293eV for C1s with an increment of 0.2eV during respectively 2.4, 1.2 and 1.2s and with a pass energy of 23.5eV. The peaks obtained are fitted by the Multipak software with a baseline and a series of peaks representing the chemical and oxidation state of the specific element. The curve-fitting is a Gaussian-lorentzian function.

To compare the effect of the laser and micro-knurling treatment on wetting, measurements of wettability were made with static contact angles using the sessile drop method [32-34]. For the wetting measurements a goniometer (model DSA030) was used. 3µL droplets of distilled water were dispensed on the sample surfaces with a 0.5mm needle from KRÜSS. For the reproducibility of results, 5 contact angle measurements were made at room conditions at 23°C and a relative humidity of 30–50%. The static contact angle mean average of these 5 measurements is then calculated and presented as the mean contact angle with a

corresponding standard deviation. The anisotropic surface texturing leads to anisotropic wettability properties. The droplet spreads in the groove direction, yielding a lower contact angle. To take into account this spreading anisotropy, the contact angles were measured in both directions (parallel and perpendicular to the grooves). So 5 measurements were made in the “perpendicular direction” and 5 were made in the “parallel direction” (Figure 5). The measurement method consisted in apparent contact angle measurements on each frame of the droplet deposition video lasting for 60 s. The videos were about 10 frames per second to have better precision on the contact angle variations. The contact angle is picked up once the droplet equilibrium state is reached, that is to say when the drop remains steady on the surface and before any evaporation regime. This state was studied and evaluated to be 10s after droplet deposition. These contact angles are calculated by the Drop Shape Analysis software using a tangent method. More precisely, a polynomial function is fitted to a section of the profile in the region of the baseline and the contact angle is determined by the slope at the 3-phase contact point at the baseline. An average of the 5 measurements done was made and reported on a graph with a Pearson standard deviation.

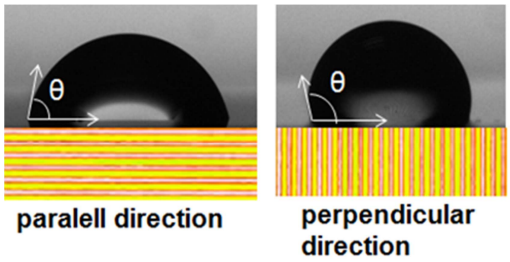

Figure 5: Contact angle measurement on parallel and perpendicular directions

3. Results and discussion

3.1 Surface morphology

Topographical confocal microscope images of both the femtosecond laser and mechanical micro-knurled surfaces are compared (Figure 6). Four typical roughness parameters (R_a, R_z, R_{sk} and R_{ku}) are analyzed and presented in Table 2. It is shown that these roughness parameters are very similar for both textured surfaces. This similarity in amplitude roughness parameters shows the ability of micro-knurling to be a good option to generate surface patterns close to the femtosecond laser process. Nevertheless, some differences can be observed on the cross-section profiles. The top and bottom of the knurled surface profile are flatter than the laser textured one. The Gaussian laser beam leads to a quasi-sinusoidal profile whereas the mechanical micro-knurling leads to patterns with larger slopes. The effect of the slopes is not evaluated in this work.

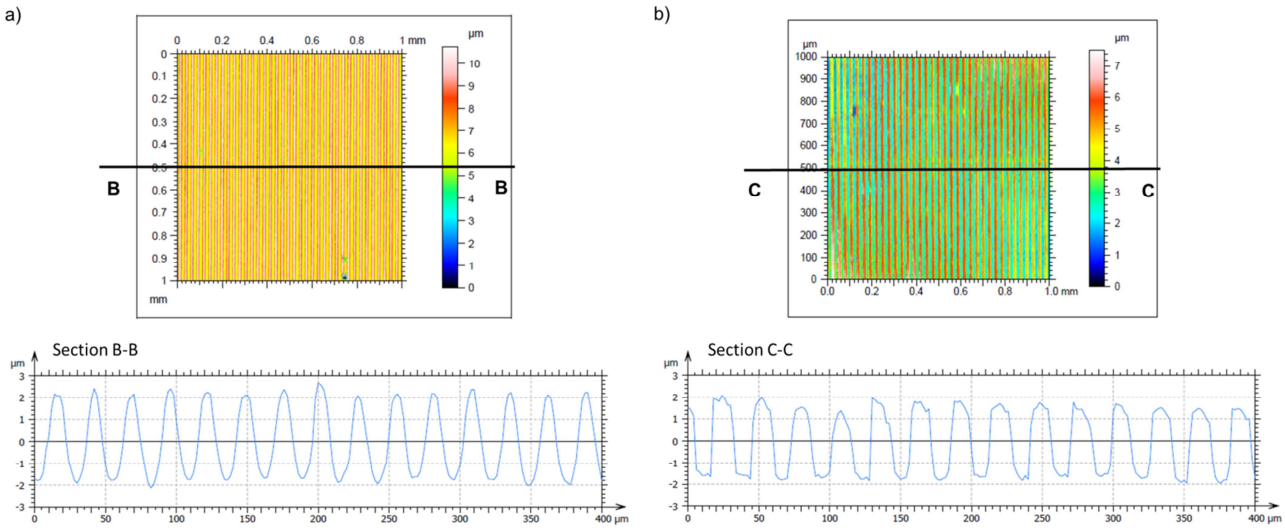

Figure 6: a) optical top-view of femtosecond laser texturing and its associated cross section profile B-B b) optical top-view of micro-knurling texturing and its associated cross section profile C-C

Roughness parameters	Surface textured by femtosecond laser	Surface textured by micro-knurling
R_a (µm)	1.4	1.3
R_z	4.3	3.5
R_{sk}	0.2	-0.1
R_{ku}	1.2	1.2
S_{dr} (%)	6.9	7.8

Table 2: Roughness parameters for surface textured by laser and surface textured by micro-knurling

3.2 Long-term surface wettability

Figure 7 shows the angle evolution over time for the reference, the femtosecond laser textured and the micro-knurled samples. As expected, the contact angles measured on the reference sample are almost time-independent with a mean value about 88°±4°.

For the micro-knurled surface, two main results may be pointed out. First, a high anisotropy of water spreading is observed. The static contact angle measured in the parallel direction 94°±4° is close to the contact angle of the reference material surface (88°±4°). In the perpendicular direction, the contact angle points out a hydrophobic behavior with a contact angle around 127°±6°. This contact angle value is explained by the pinning of the triple line on the border of the grooves [26, 35].

Secondly, the values of the contact angles measured on the micro-knurled surface present a good stability over time. No remarkable evolution over time may be measured on this mechanically textured surface.

This is a major difference with the contact angle measurements obtained on femtosecond laser textured surfaces.

Indeed, for the femtosecond laser textured surface, a significant contact angle evolution operates over time. Immediately after laser irradiation, the surface presents a hydrophilic behavior noticeable through a significant decrease in the contact angle value. The static contact angle changes from 88°±4° (reference sample) to 50°±22° in the parallel direction

during the texturing day (day0). In the perpendicular direction, such an evolution exists even if it is less significant with a contact angle of 70°±37° during day 0. Let us note that standard deviations are quite high for day 0, which points out the high reactivity of the laser freshly textured surface.

During the three days following the laser texturing process, a wetting transition is observed. An increase in the contact angle is measured. The static contact angle increases from 50°±22° to 75°±9° in the parallel direction and from 70°±37° to 103°±7° in the perpendicular direction. Then a steady state is reached in both directions. No more evolution in the contact angle is observed even for long time measurements (day 53). As explained by Kietzig *et al.* and Bizi-Bandoki *et al.*, this three-day evolution cannot be a consequence of the topography; it is a consequence of the surface chemistry rather than surface topography [16, 18]. The contact angle increase and further stabilization (after the three-day evolution) is associated to a strong decrease in the standard deviation. It may be a clue that the surface reactivity is strongly reduced three days after laser texturing.

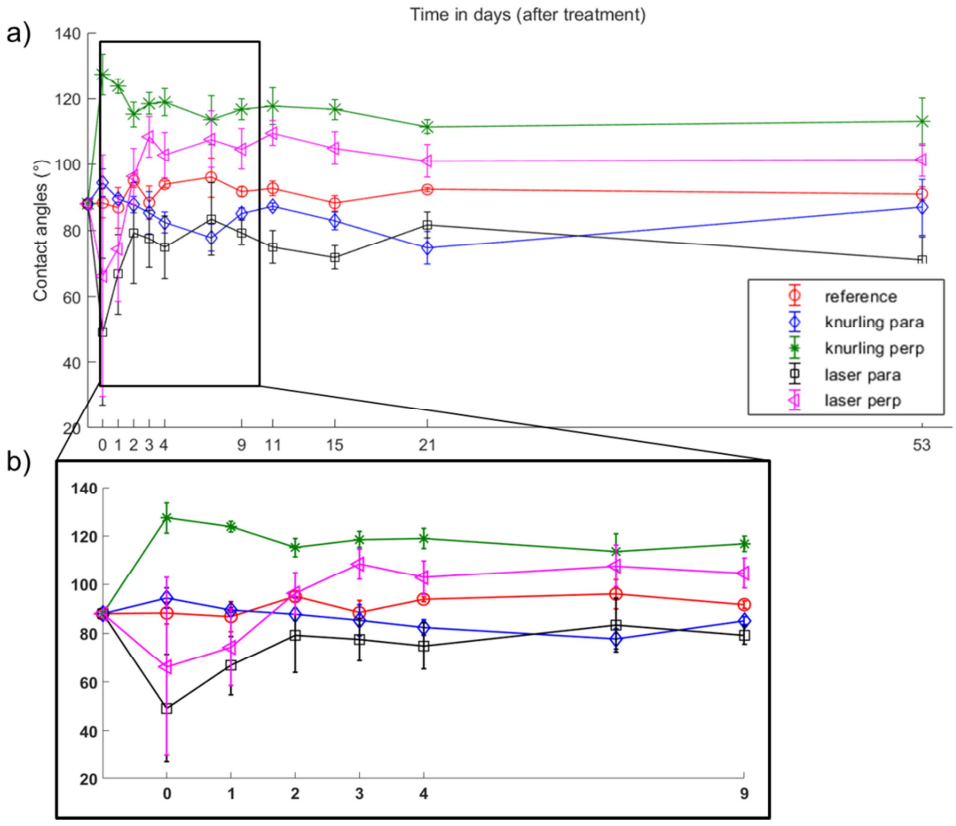

Figure 7: a) Evolution of contact angle over time b) zoom on the 3th first days.

3.3 XPS analysis

The XPS surveys of the three samples are presented in Figure 8. It may be observed from these three survey spectra that all the samples present the same chemical composition. Indeed, the three surveys spectra exhibit peaks originating from the ejection of Al2p, O1s and C1s core electrons.

The relative element percent of each element present on each surface is given in Table 3. The percent of XPS elements extracted from spectra peaks is relative. Therefore a ratio of the carbon relative percent (C_{1s}) to the oxygen relative percent (O_{1s}) was made to compare the carbon content of both different surface samples. It can be observed that the carbon content after micro-knurled texturing (C/O ratio = 4.3) is much higher than for the reference surface (C/O ratio = 1.6) (Table 3). This evolution of the relative carbon content implies that the micro-knurled environment may provide a large carbon contamination of the textured surface. This may be due to the mechanical processing environment involved for micro-knurling such as the lubricant used while operating the 5-axis machining center. However it does not play significantly on the wetting behavior (Figure 7).

On the contrary, the lower value of carbon content for the femtosecond laser textured surface (C/O ratio = 0.7) is worth noticing. The laser texturing process is associated to material removal through an ablation process. The thickness of material removal due to the femtosecond laser ablation is estimated around 2µm. Such a thickness yields a complete decontamination of the extreme surface of the sample on the one hand and allows obtaining a high reactive metallic surface on the other hand.

A high resolution XPS analysis allows a peak de-convolution and thus the calculation of relative chemical bonds involved with each element (Figure 9). Table 4 presents a summary of the atomic percent of the main bonds involved for each peak of the XPS spectra (C_{1s}, O_{1s} and Al_{2p} peaks). Focusing on the carbon peak, Figure 10 presents the time-evolution of the C-O/C-C ratio for the femtosecond laser textured surface and for the micro-knurled surface. Trend curves are added to the scatter graph for better visibility. As notified with the contact

angle evolution over time, there is almost no evolution of the chemical bond nature for the carbon peak in the case of the micro-knurled surface (C-O/C-C ratio from 0.2 to 0.1). This is not the case for the C-O/C-C ratio for the laser-textured surface. Indeed, in this case, a decrease of the ratio from 0.7 to 0.3 is measured as a function of time as the contact angles increase with time.

XPS tests reveal that the contact angle evolution is most probably explained by an extreme chemical evolution of the surface over time. According to Kietzig *et al.*, hydrophobicity can be related to the decomposition of carbon dioxide into carbon with active magnetite [16-17]. This explanation is supported by further studies of Bizi-Bandoki *et al*., Li *et al.* and Patel *et al.* [18, 36, 37]. Moreover, according to Bizi-Bandoki *et al.*, the non-polar carbon groups and graphitic carbon are hydrophobic and the carbon-oxygen bonds must be hydrophilic since the oxygen has a strong electronegativity [27]. The ratio of C-O bonds to C-C bonds can thus be considered as a good index of hydrophobicity. The present results show a decrease of this ratio over time (up to 57%). Then the hydrophobic behavior of the surface three days after texturing can be related to the increase of C-C bonds and to the decrease of C-O bonds, which corroborated the mechanism proposed by Kietzig *et al*.

Finally, it may be noticed that the C-O/C-C ratio is higher for the laser textured surface than for the micro-knurled one. This difference confirms that the micro-knurled surface is richer in carbon compared to the laser-textured one. The contamination in carbon of the mechanically textured surface is confirmed with this high-resolution analysis. The knurled surfaces do not exhibit a time-dependent wetting behavior. The ratio of C-O to C-C bonds remains very stable over time. It can be concluded that micro-knurling does not change the surface reactivity; even though a higher content of C_{1s} is observed.

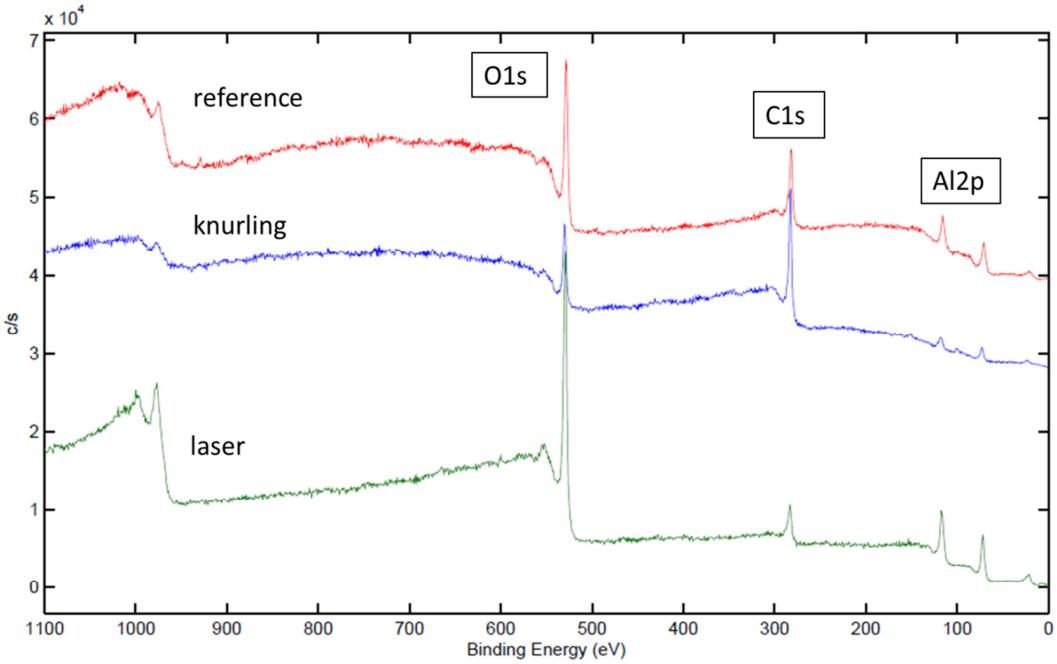

Figure 8: XPS spectra for {XPS} samples immediately after texturing

	Reference	Laser	Knurling
C_{1s}	51.2	32.7	73.9
O_{1s}	32	45.3	17
Al_{2p}	18	22	9.1
C_{1s}/O_{1s}	1.6	0.7	4.3

Table 3: Element atomic % for a reference (without treatment), a sample treated by laser and micro-knurling at day 53 after texturing.

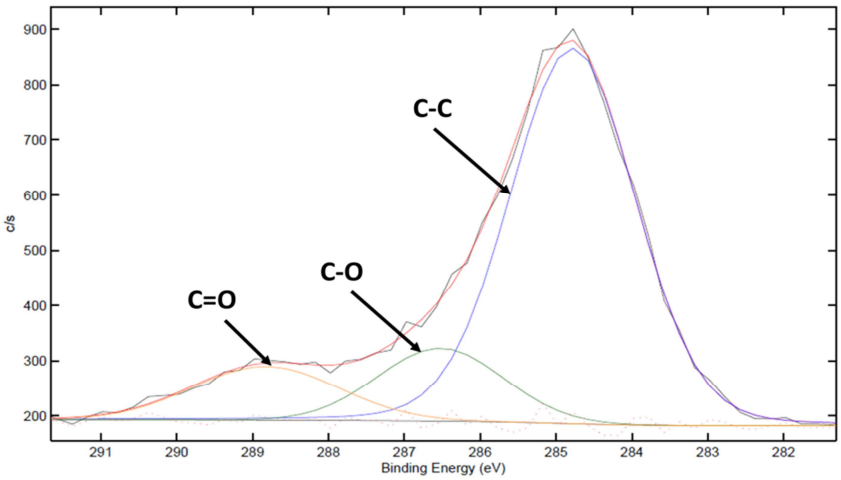

Figure 9: Deconvolution of a high resolution XPS C1s peak, 53 days after laser texturing

Elements/Compounds		Positions (eV)	Atomic %		
			reference	laser	knurling
C_{1s}	**C-C ; C-CH**	284,8	41.1	24.9	64.8
	C-O ; C-O-C	286,6	6.7	4.6	7.4
	C=O ; O-C=O	288,9	3.4	3.3	1.7
O_{1s}	**Oxides**	531,9	32	45.3	17
Al_{2p}	**Metallic Al**	72,2	2	2.5	0.7
	AlO(OH), Al_2O_3, $Al(OH)_3$	74,6	16	19.5	8.4

Table 4: Comparisons of atomic % of bonds for the reference (without treatment), the laser and the micro-knurling treatment at day 53 after texturing.

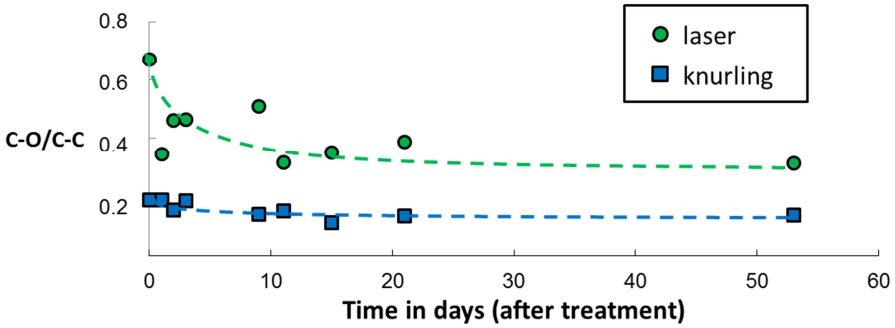

Figure 10: Evolution of ratio C-O/C-C for femtosecond laser and micro-knurling treatment function of time.

4. Conclusions

Two surface texturing processes applied on aluminum 1050 were compared using a methodology based on the surface topography, the evolution of wetting and an extreme chemical surface composition. In this study it is shown that:

- Micro-knurling is able to produce surface patterns and roughness close to those obtained using a femtosecond laser in a faster and cheaper way.
- Surfaces textured by a femtosecond laser are hydrophilic immediately after texturing and turn to a hydrophobic behavior after three days. The hydrophobic character of the femtosecond laser textured surface is then stable for 53 days after the texturing.
- The ratio of C-O bonds to C-C bonds for surfaces textured by a femtosecond laser, reveals a C-O bond decrease, which may explain the wetting behavior observed.
- Contrary to micro-knurling, femtosecond laser texturing leads to strong modifications in the surface reactivity playing on the wettability behavior.
- It may be concluded that the wetting evolution over time can be related to the evolution of the C-O/C-C ratio.

Within this work it has been shown that micro-knurling is a fast and cheap alternative to femtosecond laser processing for surface texturing. Beside its practical interest in terms of

manufacturing costs, one clear advantage of micro-knurling vs femtosecond laser is its ability to keep the surface reactivity unchanged during processing.

5. Acknowledgements

This work was supported by the LABEX MANUTECH-SISE (ANR-10-LABX-0075) of Université de Lyon, within the program “Investissements d'Avenir” (ANR-11-IDEX-0007) operated by the French National Research Agency (ANR) and by l’EQUIPEX MANUTECH-USD (ANR-10-EQPX-36-01).

We would like to convey our gratitude to Jules GALIPAUD and Thierry LE MOGNE for their XPS expertise.

6. References

[1] M. Callies Reyssat, Splendeur et misère de l'effet lotus, PhD, Université Pierre et Marie Curie, Paris VI (2007).

[2] W. Barthlott, C. Neinhuis, Purity of the sacred lotus or escape from contamination in biological surfaces, Planta **202** (1) (1997) 1-8.

[3] P.G. de Gennes, Wetting: statics and dynamics, Review of modern physics, **57** (3) (1985) 827-863.

[4] G. Huber, S.N. Gorb, N. Hosoda, R. Spolenak, E. Arzt, Influence of surface roughness on gecko adhesion, Acta Biomaterialia **3** (2007) 607–610.

[5] J. Xie, M. Li, W. Huang, X. Wang, Key parameters of biomimetic patterned surface for wet adhesion, International Journal of Adhesion and Adhesives **82** (2018) 72–78.

[6] U. Hermens, S.V. Kirner, C. Emonts, P. Comanns, E. Skoulas, A. Mimidis, H. Mescheder, K. Winands, J. Krüger, E. Stratakis, J. Bonse, Mimicking lizard-like surface structures upon ultrashort laser pulse irradiation of inorganic materials, Appl. Surf. Sci.**418** (2016) 499-507.

[7] T. Ibatan, M.S. Uddin, M.A.K. Chowdhury, Recent Development on Surface Texturing in Enhancing Tribological Performance of Bearing Sliders, Surface & Coatings Technology **272** (2015) 102-120.

[8] S. Valette, E. Audouard, R. Le Harzic, N. Huot, P. Laporte, R. Fortunier, Heat affected zone in aluminum single crystals submitted to femtosecond laser irradiations, Applied Surface Science **239** (2005) 381-386.

[9] S. Valette, P. Steyer, L. Richard, B. Forest, C. Donnet, E. Audouard, Influence of femtosecond laser marking on the corrosion resistance of stainless steels, Applied Surface Science **252** (2006) 4696-4701.

[10] P. Steyer, S. Valette, B. Forest, J-P. Millet, C. Donnet, E. Audouard, Surface modification of martensitic stainless steels by laser marking and its consequences regarding corrosion resistance, Surface Engineering **22** (3) (2006) 167–172.

[11] R.A. Ganeev, T.Q. Jia, Nanostructuring of Semiconductor Surfaces under the Action of Femtosecond Pulses, Optics and Spectroscopy **105** (1) (2008) 141-146.

[12] B. Wu, M. Zhou, J. Li, K. Ye, G. Li, L. Cai, Superhydrophobic surfaces fabricated by microstructuring of stainless steel using a femtosecond laser, Applied Surface Science **256** (2009) 61-66.

[13] M.N.W. Groenendijk, J. Meijer, Surface Microstructures obtained by Femtosecond Laser Pulses, Annals of the CIRP **55** (1) (2006).

[14] G. Pardal, S. Meco, A. Dunn, S. Williams, S. Ganguly, D.P. Hand, K.L. Wlodarczyk, Laser spot welding of laser textured steel to aluminum, Journal of Materials Processing Technology **241** (2017) 24–35.

[15] K. Goya, Y. Yamachoshi, Y. Fuchiwaki, M. Tanaka, T. Ooie, K. Abe, M. Kataoka, Femtosecond laser direct fabrication of micro-grooved textures on a capillary flow immunoassay microchip for spatially-selected antibody immobilization, Sensors and Actuators B **239** (2017) 1275–1281.

[16] A.-M. Kietzig, M.N. Mirvakili, S. Kamal, P. Englezos, S.G. Hatzikiriakos, Laser-Patterned Super-Hydrophobic Pure Metallic Substrates: Cassie to Wenzel Wetting Transitions, J. Adhesion Sci. Technol. **25** (2011) 2789–2809.

[17] A.-M. Kietzig, S.G. Hatzikiriakos, P. Englezos, Patterned Superhydrophobic Metallic Surfaces, Langmuir **25** (8) (2009) 4821–4827.

[18] P. Bizi-Bandoki, S. Valette, E. Audouard, S. Benayoun, Time dependency of the hydrophilicity and hydrophobicity of metallic alloys subjected to femtosecond laser irradiations, Applied Surface Science **273** (2013) 399– 407.

[19] C. Sciancalepore, L. Gemini, L. Romoli, F. Bondioli, Study of the wettability behavior of stainless steel surfaces after ultrafast laser texturing, Surface & Coatings Technology **352** (2018) 370-377.

[20] Popular Mechanics Magazine, **98** (July 1952) 191-93.

[21] W. Willard, J.D. Munter, Knurl roll design for stable rotogravure coating, Chemical Engineering Science **38** (8) (1983) 1309-1314.

[22] H. Coban, A.K.M. De Silva, D.K. Harrison, Mill-knurling as an alternative to laser welding for automotive drivetrain Assembly, CIRP Annals Manufacturing Technology **58** (2009) 41–44.

[23] K.J. Kubiak, M.C.T Wilson, T.G. Mathia, Ph. Carval, Wettability versus roughness of engineering surfaces, Wear **271** (2011) 523-528.

[24] J. Bico, C. Tordeux, D. Quéré, Rough wetting, Europhys. Lett. **55** (2) (2001) 214–220.

[25] D. Quéré, Rough ideas on wetting, Physica A **313** (2002) 32-46.

[26] A. Marchand, Mouillage statique et dynamique: Influences géométriques aux échelles moléculaires. Mécanique des fluides, PhD, Université Paris-Diderot, Paris VII (2011).

[27] P. Bizi-Bandoki, S. Benayoun, S. Valette, B. Beaugiraud, E. Audouard, Modifications of roughness and wettability properties of metals induced by femtosecond laser treatment, Applied Surface Science **257** (2011) 5213–5218.

[28] J-B Sauvage, Caractérisation et modélisation de l'adhérence dans les assemblages collés, Chimie des matériaux, PhD, L'Université de Haute Alsace (2015).

[29] A.B.D Cassie and S. Baxter, Transaction of the Faraday Society **40** (1944) 546–551.

[30] Y.R. Kolobov, Superhydrophylic textures fabricated by femtosecond laser pulses on sub-micro-and nano-crystalline titanium surfaces, Laser Phys. Lett. **11** (2014) 125602.

[31] C. Ma, S. Bai, Y. Meng, X. Peng, Hydrophilic control of laser micro-square-convexes SiC surfaces, Materials Letters **109** (2013) 316–319.

[32] Y.Yuan, T.R. Lee, Contact Angle and Wetting Properties. In: Bracco G., Holst B. (eds) Surface Science Techniques. Springer Series in Surface Sciences, vol 51. Springer, Berlin, Heidelberg, 2013.

[33] D. Quéré, Wetting and Roughness, Annual Review of Materials Research **38** (2008) 71-99.

[34] J. Bico, U. Thiele, D. Quéré, Wetting of textured surfaces, Colloids and Surfaces A: Physicochem. Eng. Aspects **206** (2002) 41–46.

[35] E.Bormashenko, Progress in understanding wetting transitions on rough surfaces, Advances in Colloid Interface Science **222** (2015) 92-103.

[36] X. Li, C. Yuan, H. Yang, J. Li, W. Huang, D. Tang, Q. Xu, Morphology and composition on Al surface irradiated by femtosecond laser pulses, Applied Surface Science **256** (2010) 4344-4349 .

[37] D.S Patel, A. Singh, K. Balani, J. Ramkumar, Topographical effects of laser surface texturing on various time-dependent wetting regimes in Ti6Al4V, Surface & Coatings Technology **349** (2018) 816-829.